

## Article

# Physical Similarity Simulation of Deformation and Failure Characteristics of Coal-Rock Rise under the Influence of Repeated Mining in Close Distance Coal Seams

Pengze Liu <sup>1</sup>, Lin Gao <sup>1,2,3,4,\*</sup> , Pandong Zhang <sup>1</sup>, Guiyi Wu <sup>1,3</sup>, Yongyin Wang <sup>1,3</sup>, Ping Liu <sup>1,3</sup>, Xiangtao Kang <sup>1,3</sup> , Zhenqian Ma <sup>1,3</sup> , Dezhong Kong <sup>1,3</sup> and Sen Han <sup>1,3</sup>

- <sup>1</sup> College of Mining, Guizhou University, Guiyang 550025, China; liupengze0205@163.com (P.L.); zpdznh@163.com (P.Z.); gywu@gzu.edu.cn (G.W.); yywang2@gzu.edu.cn (Y.W.); pliu1@gzu.edu.cn (P.L.); xiaokangedu@163.com (X.K.); zqma@gzu.edu.cn (Z.M.); dzkong@gzu.edu.cn (D.K.); shan1@gzu.edu.cn (S.H.)
- <sup>2</sup> Coal Mine Roadway Support and Disaster Prevention Engineering Research Center, Beijing 100083, China
- <sup>3</sup> National & Local Joint Laboratory of Engineering for Effective Utilization of Regional Mineral Resources from Karst Areas, Guiyang 550025, China
- <sup>4</sup> Key Laboratory of Mining Disaster Prevention and Control, Qingdao 266590, China
- \* Correspondence: lgao@gzu.edu.cn



**Citation:** Liu, P.; Gao, L.; Zhang, P.; Wu, G.; Wang, Y.; Liu, P.; Kang, X.; Ma, Z.; Kong, D.; Han, S. Physical Similarity Simulation of Deformation and Failure Characteristics of Coal-Rock Rise under the Influence of Repeated Mining in Close Distance Coal Seams. *Energies* **2022**, *15*, 3503. <https://doi.org/10.3390/en15103503>

Academic Editors: Jing Li, Yidong Cai, Lei Zhao and Manoj Khandelwal

Received: 9 March 2022

Accepted: 5 May 2022

Published: 11 May 2022

**Publisher's Note:** MDPI stays neutral with regard to jurisdictional claims in published maps and institutional affiliations.



**Copyright:** © 2022 by the authors. Licensee MDPI, Basel, Switzerland. This article is an open access article distributed under the terms and conditions of the Creative Commons Attribution (CC BY) license (<https://creativecommons.org/licenses/by/4.0/>).

**Abstract:** Aiming at the problem that it is difficult to achieve accurate laying of model and precise excavation of roadways in special surrounding rock structure roadway according to conventional physical similarity simulation, which reduces the reliability of experimental results. An accurate laying of model and precise excavation of roadway method, named “labeling positioning and drawing line, presetting roadway model” (LPDLPRM), was proposed. The physical similarity simulation of deformation and failure characteristics of surrounding rock of coal-rock rise, under the influence of repeated mining in close distance coal seams, was carried out based on the method and infrared detection. The results show that the coal-rock rise in close distance coal seams was affected by repeated mining disturbances, and the surrounding rock of coal-rock rise was characterized by obvious asymmetric deformation, specific for the stress and strain near the coal pillar were higher than that of other parts, and cracks near the coal pillar were denser than other parts; when the coal seam is mined in which the coal-rock rise is located, the stress concentration of the surrounding rock near the rise was weakened by mining pressure relief in the upper coal seam; the stress concentration of the surrounding rock near the rise increases when the coal and the lower coal seam are mined, and the stress on the right side (coal pillar side) near the coal-rock rise was the most concentrated. Therefore, it is important to take measures to strengthen support near the coal pillar and to control asymmetric deformation when the coal-rock rise is influenced by repeated mining.

**Keywords:** similar simulation test; precise excavation of roadway; repeated mining; coal-rock roadway; infrared thermal image

## 1. Introduction

Mineable coal seams in Guizhou Province of China are mainly characterized by complex geological structure, close distance, and thin and medium thick coal seams [1,2]. Compared with a single thick coal seam, the mining process in Guizhou is mostly accompanied by violent mine pressure and continuous large deformation of surrounding rock [3]. These are the important factors to restrict the improvement of the coal mine safety situation and production efficiency in Guizhou. Therefore, it is urgent to further reveal the deformation characteristics of surrounding rock and to provide the scientific basis for support design in Guizhou.

In general, the commonly used research methods in mining engineering include theoretical analysis, numerical simulation, physical similarity simulation, etc. [4,5], while

physical similarity simulation is widely used in the field of mining engineering, because it has some obvious advantages, such as intuitive test effect, short test cycle, high simulation degree and easy operation [6–13].

For example, Lin et al. [14] simulated roadway excavation in a coal mine, used a self-made model to build a test model, which was controlled by microcomputer and employing an electro-hydraulic servo universal testing machine to load. Chen et al. [15] simulated roadway excavation with high geostress, which was supported by an anchor used self-made true three-dimensional loading model test system. Pornkasem Jongpradist et al. [16] studied the fracture mechanism of surrounding rock for high internal pressure roadway through establishing physical similarity model. Yan et al. [17] studied the dynamic failure process of surrounding rock from stability to instability for a horizontal extra thick coal seam through physical similarity simulation test, and revealed the stress and displacement characteristics of a fully mechanized mining roadway. Hui et al. [18] adopted a manual opening model center to simulate tunnel excavation in a physical similarity simulation test. Mishra Swapnil et al. [19] studied the behavior and pattern of tunnel damage subjected to the different dynamic loading conditions by a similar simulation. Shan et al. [20] adopted the self-developed new simulation test device of roadway support, which can apply dynamic and static load, and studied the influence of dynamic and static load on roadway deformation law by comparison. Chang et al. [21] reproduced a high stress environment of deep roadway through applying different pressure on roof, floor and both sides of the roadway with a four-way loading simulation test bench. Wook and Lee [22] investigated pile load distribution and ground behavior due to tunnelling below a grouped pile using a laboratory model test. Li et al. [23] studied the failure characteristics of a roadway under uniaxial and biaxial compression using a self-developed biaxial loaded roadway simulation test system equipped with a small and medium-sized motor. Yuan et al. [24] proposed a new method of similar material simulation test combined with orthogonal test and multiple regression analysis, and studied the protective effect of upper protective layer mining of a steeply inclined coal seam with variable interval using this method. Wang et al. [25] explored the dynamic response and impact failure characteristics of coal and rock mass under a steeply inclined extra-thick coal seam through the physical simulation experiment with static and dynamic coupling loading. Idinger Gregor et al. [26] investigated some aspects of the collapse at tunnel face for different overburden pressures on a small-scale tunnel model in a geotechnical centrifuge. He et al. [27] committed to the simulation of a roadway excavation in the geologically horizontal strata at great depth based on a physical modeling test. Li et al. [28] investigated the evolution laws of floor rock fracture under the mining dynamic loading effects by a similar simulation test. Ren et al. [29] studied the characteristics of the breaking process of overburden rocks in shallow coal workface through physical similarity simulation. Shi et al. [30] studied the movement law, failure mechanism and fracture evolution of overlying strata of gob-side entry driving in thick coal seam by combining physical model test and numerical simulation. Berthoz Nicolas et al. [31] studied mechanisms of face collapse and face blow-out of tunnels driven in soft grounds with pressurized shield tunnel boring machine with original laboratory reduced-scale model. Feng et al. [32] studied the failure law of rock during coal mining by physical similar material simulation experiment. Xue et al. [33] simulated the movement and fracture evolution of the overlying strata after the coal seam is extracted. Yang et al. [34] studied the development of mining stress and the effect of large height upward mining pressure relief gas using physical similarity simulation. Zhang et al. [35] analyzed the displacement, strain and vertical stress field of surrounding rock near the fault, and determined the influence of coal pillar width by similar simulation combined with digital speckle.

Summarizing above literature, it was found that most of the existing studies on the deformation characteristics of roadway surrounding rock and pressure behavior using physical similarity simulation focused on roadways in nearly horizontal thick coal seam. However, coal-rock rise widely used in close distance, thin and medium thick coal seams in Guizhou Province of China. Due to the heterogeneity of surrounding rock structure

and the existence of the coal–rock interface, the mechanical properties of the surrounding rock were influenced, and it was difficult to achieve accurate laying of model and precise excavation of roadways. Though physical similarity simulation is widely used to study the mine pressure behavior of roadways, the relevant literature is rarely mentioned on close distance, thin and medium thick coal seams. To further intuitively reveal the deformation characteristics of coal–rock rise under the influence of repeated mining in close distance coal seams, a physical similarity simulation test method of accurate laying of model and precise excavation of roadway was proposed. Combined with infrared thermal detection means, physical similar simulation experiment research was conducted for the roadways of special surrounding rock structures.

## 2. The Proposition of Accurate Laying and Excavation Method of Similarity Simulation Model in Roadway of Special Surrounding Rock Structure

Special surrounding rock structures such as inclined coal and rock strata and coal–rock roadways were common in Guizhou Province of China [36–38]. It was difficult to achieve precise laying of the conventional physical similarity test model and precise excavation of roadway in these coal and rock strata. That resulted in the physically similar experiment results that were not accurate, and its application was limited. Based on this, the research group proposed an accurate laying of model and precise excavation of roadway test method named “labeling positioning and drawing line, presetting roadway model” (LPDLPRM).

### 2.1. Basic Process of the Test Method

This test method mainly consists of determining similar materials and its ratio, model design, installing and debugging test bench, mixing similar materials, making roadway model, labeling positioning and drawing line, laying model, presetting roadway model, maintaining model and others. Among these, making roadway model, labeling positioning and drawing line, and presetting roadway model are the core contents of this method. The detailed process are as follows:

#### 1. Making roadway model.

The roadway model is the core component of the accurate laying of model and precise excavation of roadway method. The roadway model consists of an inner frame produced by  $\Phi 5$  mm steel and PC plastic sheet surrounding the inner frame. In order to ensure the smooth pull out of the model from coal and rock strata and to reduce the large friction when roadway excavation is conducted in the later stage of the test, the PC plastic sheet is brushed with oil. This model is shown in Figure 1.



**Figure 1.** Composition of roadway model.

#### 2. Labeling positioning and drawing line.

According to the model design drawing, the laying position of each coal and rock strata on the baffle plate of the test bench are drawn. Additionally, the positioning prompt labels of roadway model and test components such as pressure box are affixed on corresponding position where both sides and the baffle at the back of the model. That can ensure the accurate laying of subsequent all coal and rock strata and roadway model. Then, labeling the names of all coal and rock strata, and drawing the boundary line of each coal and rock strata, drawing the position of each stress sensors and the outline of the roadway.

3. Presetting roadway model.

When the model is laid to the corresponding labels of the outline of the roadway, the roadway model is embedded according to the calibration position, the pressure boxes are buried according to the positioning labels, and a layer of edible oil is brushed on the outside of the roadway model. After the laying and maintenance are completed, the roadway model is pulled out to simulate the excavation of the roadway.

2.2. The Advantages of this Experimental Method

Compared to the traditional experimental method, through the labeling the roadway outline and coal and rock boundary in advance, this method can realize not only the accurate laying of model in coal and rock strata (especially the inclined coal and rock strata), but also the precise excavation of roadway. At the same time, through the position labels, pressure sensors and others can be accurately embedded to ensure the location of pressure sensors consistent with the design scheme, so that the test data collected is highly reliable and accurate. This method aims to solve the problems of the uneven thickness of coal and rock strata, the irregular outline of excavated roadway and unreliability monitoring data of the physical similarity simulation experiment in special surrounding rock structure.

3. Overview of the Project

A coal mine in Guizhou Province of China is characterized by complicated geological structures where faults and folds widely existed. Its minable coal seams are typical close distance coal seams, which roof and floor are mostly mudstone, argillaceous siltstone and other soft rocks. Rise for transportation is located in 17# coal and its floor, and about two-thirds of which cross section is in 17# coal. The roadway is driven along the roof of 17# coal. The average thickness and dip angle of 17# coal are 2.5 m and 20°, respectively. The cross section of the roadway is a straight wall and semicircular arch with a lower width of 5.5 m and middle height of 3.3 m. It is a typical coal-rock roadway. The position relation of each coal and rock strata and rise for transportation is shown in Figure 2.

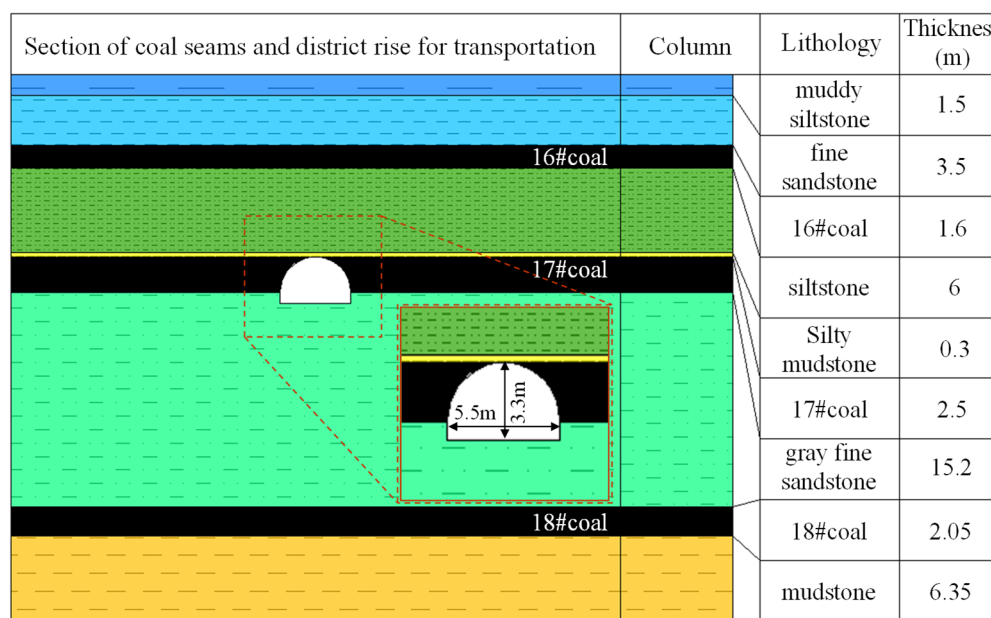


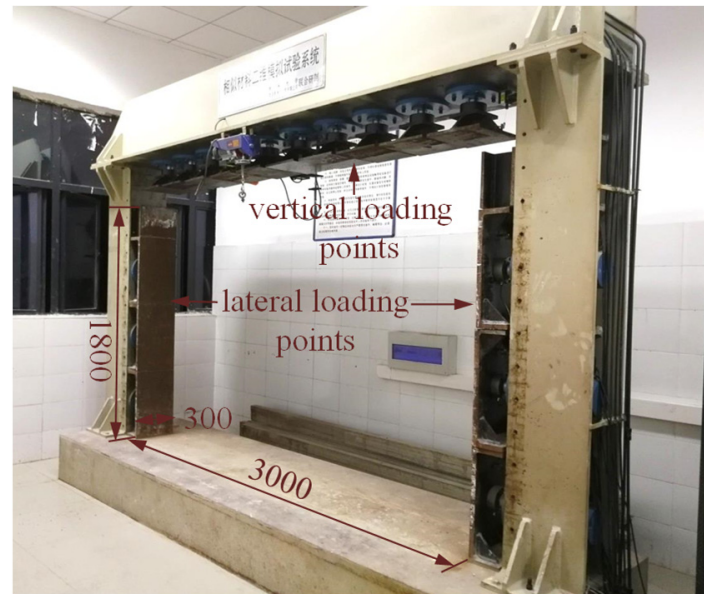
Figure 2. Strata histogram in this research.

4. Experiment Plan of the Physical Similarity Simulation

4.1. Test Equipment and Test System

The test device is the QKX-EW-2 two-dimensional physical similarity simulation test bench (Figure 3) with a length of 3000 mm, width of 300 mm and height of 1800 mm. There are 10 vertical loading points, and the maximum pressure/load that can be applied

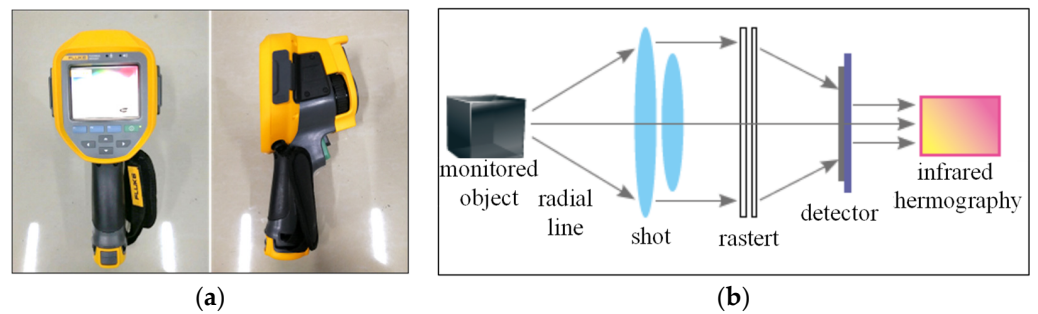
is 1 MPa/1000 kN. Three lateral loading points are arranged on the left sides and three on the right sides with maximum loading pressure/load being 1 MPa/600 kN for each loading point, and pressure of the loading system is 15 MPa. The loading plate is pushed by the oil cylinder to realize vertical and lateral loading. Among them, the dimensions of the 10 vertical active loading plates are all 300 mm × 300 mm (length × width). The dimensions of the three lateral loading plates on the left or right sides are 500 mm × 300 mm (height × width), and the rated voltage/power is 380 V/55 kW. They can be used at −10–65 °C. At the same time, in order to reduce the influence of boundary effect, the excavation area is arranged near the diagonal of the test bench as far as possible.



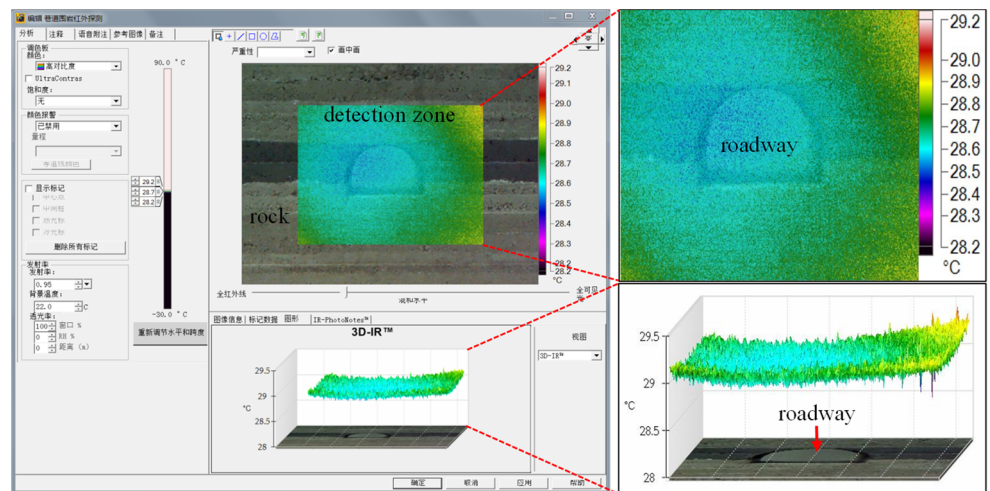
**Figure 3.** QKX-EW-2 two-dimensional physical similarity simulation test bench.

The high-definition and high-speed digital shooting system was adopted for data collection. Using CanonEOS750D high-definition digital camera controlled by mobile phone through wireless connection to track, shoot and record changes of surrounding rock cracks at key moments. Using high-speed camera Qianyanlang 2F04 equipped with EF-200LED lighting to capture the instantaneous cracks and deformation of the surrounding rock. Using SONY full HD digital camera to record the whole process of the experiment and to ensure every detail of experiment to be recorded.

As the relationship between surrounding rock stress, strain and surrounding rock surface infrared radiation can be expressed qualitatively. Additionally, with the increase of load, the infrared radiation temperature is higher [39–45], Fluke Ti450PRO infrared thermal imager was used for infrared detection of roadway surrounding rock during the experiment. The temperature measurement range of Fluke Ti450PRO infrared thermal imager is −20–1200 °C, the thermal sensitivity is 0.025 °C (30 Mk), and the image resolution is 640 × 480. The principle of Fluke Ti450PRO infrared thermal imager is to passively receive the infrared radiation (heat) from the measured target through non-contact nondestructive detection and to convert this heat into a visual image (IR image) with temperature data, which is shown in Figure 4. The image data were imported into SmartView4.3 professional infrared thermal analysis software (Figure 5) for data processing and analysis, then the two-dimensional and three-dimensional temperature fields of the detection object were obtained, which can be used to analyze the stress state of the surrounding rock indirectly.



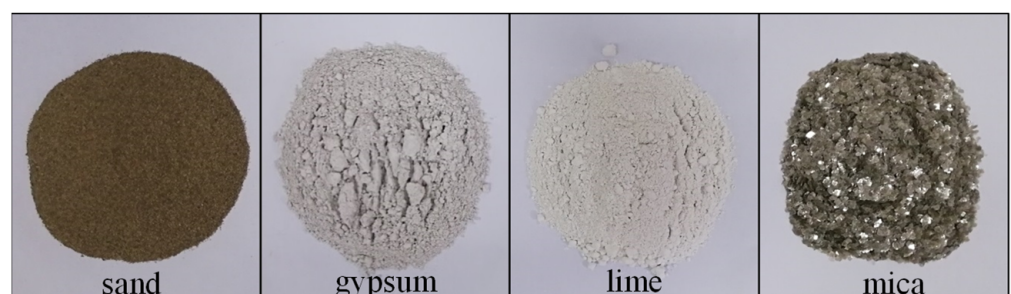
**Figure 4.** Infrared thermal imager and its working principle. (a) Infrared thermal imager; (b) and working principle.



**Figure 5.** Infrared thermal analysis software. (Its function keys only provide Chinese display).

#### 4.2. Experimental Materials and Making Similar Models

1. Determination of similar materials and ratio number. The selection of similar materials and the determination of reasonable ratio number are crucial to obtain accurate and reliable results of similar simulation experiment. According to the mechanical parameters of actual coal and rock strata and similarity theory, the geometric similarity ratio of the model  $C_l = 25$ , the density similarity ratio  $C_\gamma = 1.5$ , the stress similarity ratio  $C_p = 37.5$ , and the time similarity ratio  $C_t = 5$  were chosen. Similar materials (Figure 6) choose sand as aggregate, lime and gypsum as cementing materials, and mica powder was spread between layers of coal and rock to simulate bedding. According to the calculation method of the strength value of coal and rock mass simulated by similar materials, the strength test of similar materials with different proportions was carried out for the main coal and rock strata. After repeated adjustment, the reasonable ratio number of similar materials for each coal and rock strata was obtained, as shown in Table 1.

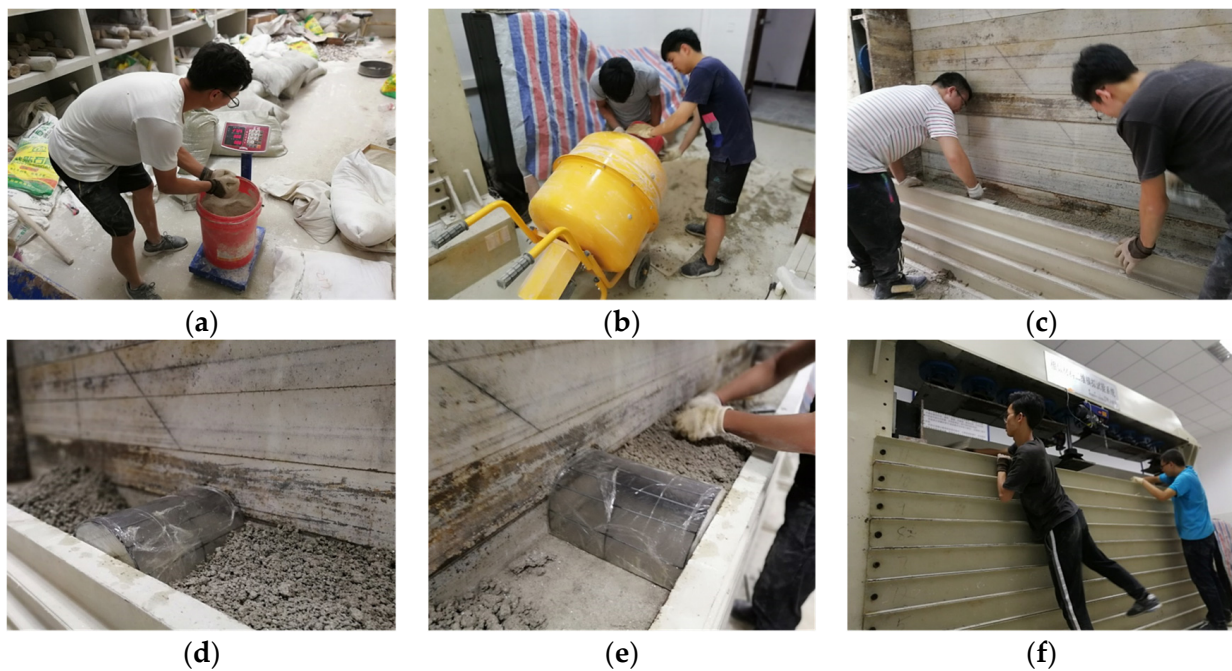


**Figure 6.** Main similar materials.

**Table 1.** Similar material ratio and mechanical parameters.

Rock Stratum Number	Thickness (m)	Lithology	Proportion Number	Model Thickness (cm)	Density (g/cm <sup>3</sup> )	Lamination Thickness (cm)	Layer Number	Weight of Water	Compressive Strength (MPa)
9	1.5	muddy siltstone	355	6	1.58	2.0	3	1/9	0.63
8	3.5	fine sandstone	473	14	1.55	2.0	7	1/9	0.57
7	1.6	16#coal	773	6.4	0.93	2.0	3	1/9	0.08
6	6	siltstone	373	24	1.70	2.0	12	1/9	0.75
5	0.3	silty mudstone	582	1.2	1.46	1.2	1	1/9	0.51
4	2.5	17#coal	773	10	0.93	2.0	5	1/9	0.08
3	15.2	gray fine sandstone	472	60.8	1.55	2.0	30	1/9	0.56
2	2.05	18#coal	773	8.2	0.93	2.0	4	1/9	0.08
1	6.35	mudstone	573	25.4	1.42	2.0	13	1/9	0.46

- 2 Model design. According to the size of roadway, the true thicknesses of each coal and rock strata, the geometric similarity ratio, the size of test bench, and others, the size of the roadway model and its thicknesses of each coal and rock strata were determined, then the model design diagram was drawn. Before the model was laid, the quality of sand and lime in each layer was calculated according to the real thicknesses of each coal and rock strata, geometric similarity ratio, model test bench size, similar material density and ratio number. Then, the preparation of weighing ratio and mixing of similar materials was completed.
- 3 LPDLPRM. The positioning labels of the roadway model and pressure box were put on the test bench according to the drawing, the separation lines of the coal and rock strata were drawn, mark the names of the coal seam and rock strata. Then, the coal seams and rock strata were laid, respectively, using similar materials which had been matched. The coal seams and rock strata were laid one by one and compacted every 5 cm. In order to make the model layered obviously, a layer of mica powder was evenly spread on it as a weak layer after each strata of coal and rock was laid. When the model was laid to the marked position, the roadway model that has been made was embedded to the marked position. We continued these procedures until the model laying was completed. The test process is shown in Figure 7.

**Figure 7.** The process of making model. (a) Weighing ratio; (b) mixing materials; (c) laying model; (d) presetting of roadway model; (e) compacted materials; and (f) laying upper part of model.

- 4 Maintenance of model. Three days after the model was laid, the fixed steel plates in front and back of the model were removed. When the whole model was dry, there were no water marks, and the whole was gray, pressing hard on its surface will not produce obvious depression, indicating that the experimental requirements were met. Then, the dense observation grids were drawn to ensure accurately record the variation characteristics of surrounding rock cracks during roadway excavation. Thus far, the test model was completed, which is shown in Figure 8.



**Figure 8.** Final drawing of test model.

#### 4.3. Process of the Experiment

The experiment was started when the model was static air-dried to achieve the desired effect and the model strength reached the design requirements. According to the buried depth and stress similarity ratio of the roadway, evenly and gradually vertical load applied on the top of the model, kept the oil pressure of each loading plate stabilized, and kept the load constant, then carried out the roadway excavation (the preset roadway model was extracted). The excavation position was in the middle of coal–rock combination body of 17# coal and lower rock. During the process of the roadway excavation, a high-definition camera was used to capture the instantaneous cracks and deformation of the surrounding rock, and a camera was used to record the whole test until the surrounding rock deformation tended to be stable.

### 5. Experiment Results and Analysis

#### 5.1. Evolution Characteristics of Surrounding Rock Cracks

During the experiment, roadway excavation was simulated by extracting the preset roadway model, and the minable 16#, 17# and 18# coal seams were simulated by this kind of manual excavation. At the same time, the high-definition digital camera wireless connected to mobile phone was used to track and record the fracture situation of surrounding rock at key moment. The obtained images were imported into AutoCAD in raster image format to obtain the sketch map of fracture distribution of surrounding rock. The results show that after the 16# coal was mined, only a few fine cracks were generated away from the roadway; when the 17# coal (the coal seam in which the coal-rock rise was) was mined, a large range of cracks were produced on the roof and the upper right of the roadway; when the 18# coal was mined, the cracks on the right side of the roadway floor continued to extend downward. The distribution of cracks in surrounding rock of the roadway was asymmetric in the form of left thin and right dense, and the surrounding rock of roadway showed obvious asymmetric deformation characteristics. The crack distribution and evolution sketch of surrounding rock of the coal-rock roadway during the experiment were shown in Figure 9.

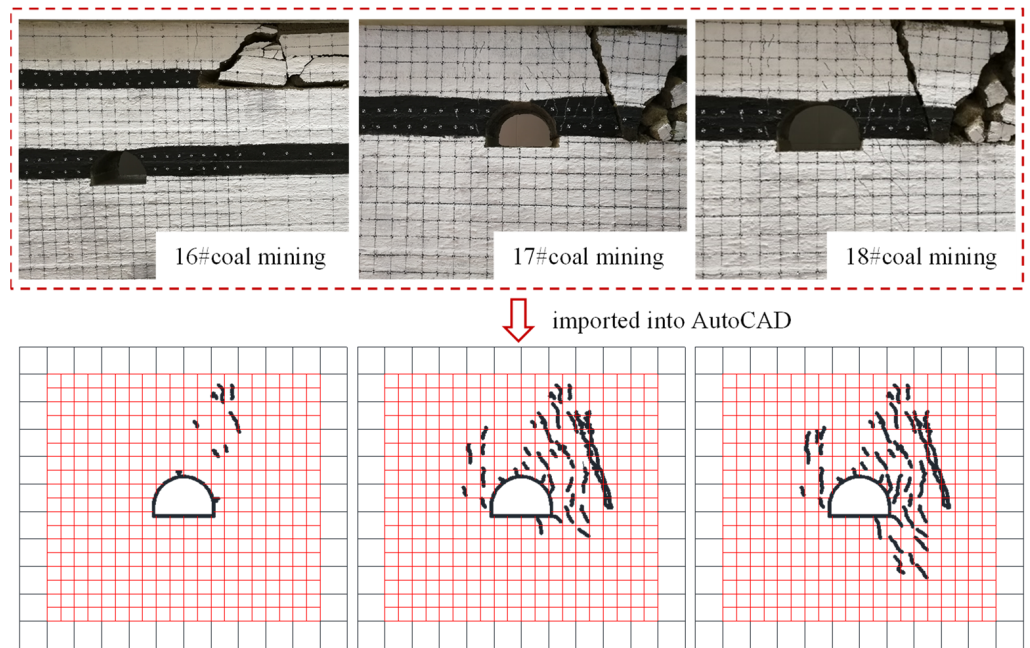


**Figure 9.** Sketch of fracture distribution and evolution of surrounding rock of coal-rock district rise.

5.2. Analysis of the Results of Infrared Thermal Imager Detection

Under the influence of mined and non-mined roadway surrounding rock for different coal seams (16#, 17#, 18#), the plane temperature field of roadway surrounding rock, large-scale three-dimensional temperature field of roadway surrounding rock, and the temperature changes at different positions of roadway surrounding rock in different coal seam mining were shown in Figures 10–12.

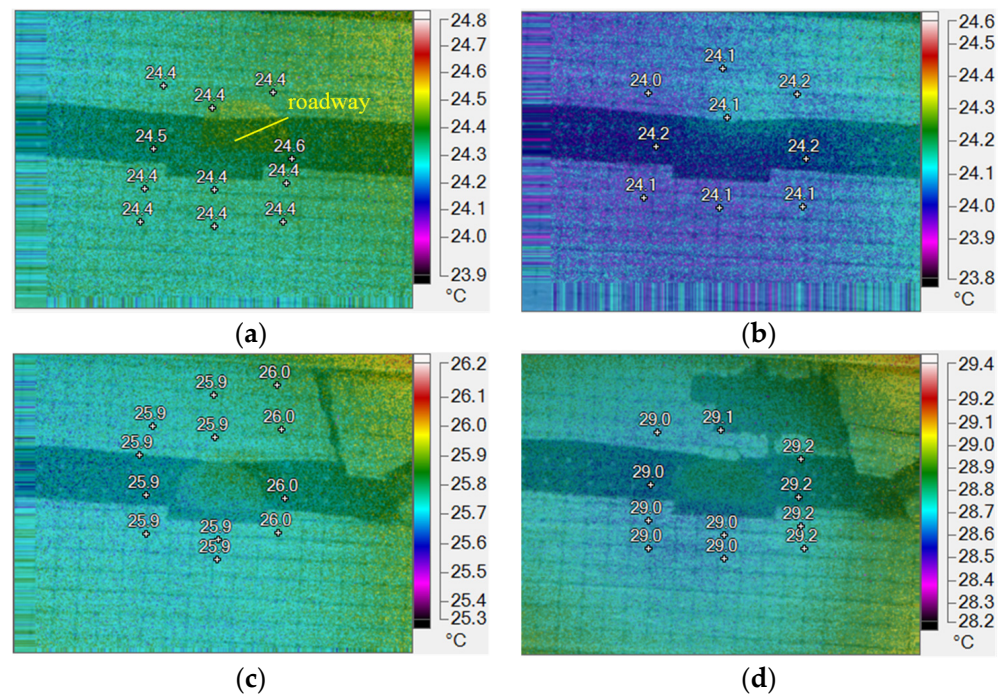


**Figure 10.** Plane temperature field of surrounding rock in mining roadway in different coal seams. (a) No-mining; (b) 16# coal mining; (c) 17# coal mining; and (d) 18# coal mining.

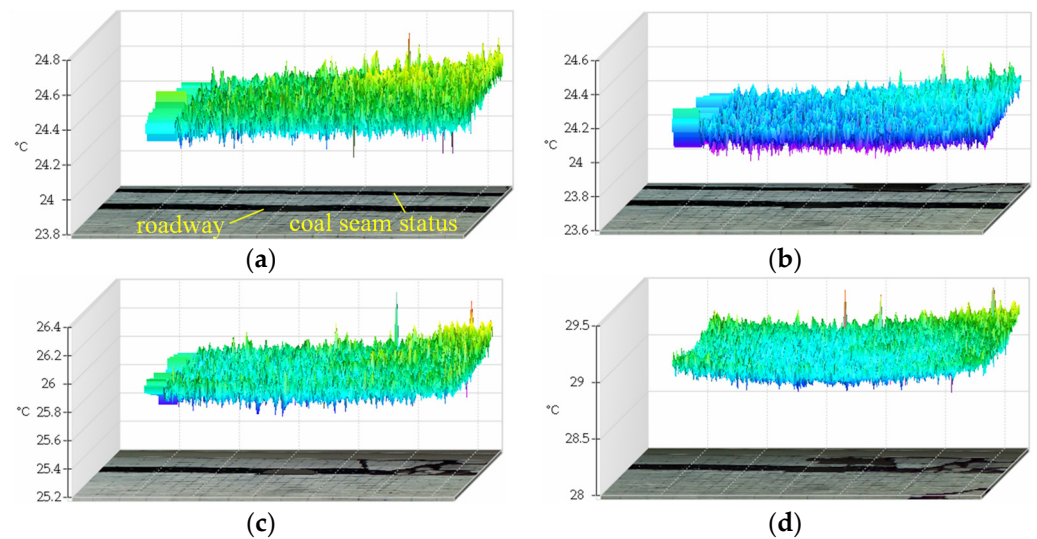


**Figure 11.** Three-dimensional temperature field of surrounding rock in mining roadway in different coal seams. (a) No-mining; (b) 16# coal mining; (c) 17# coal mining; and (d) 18# coal mining.

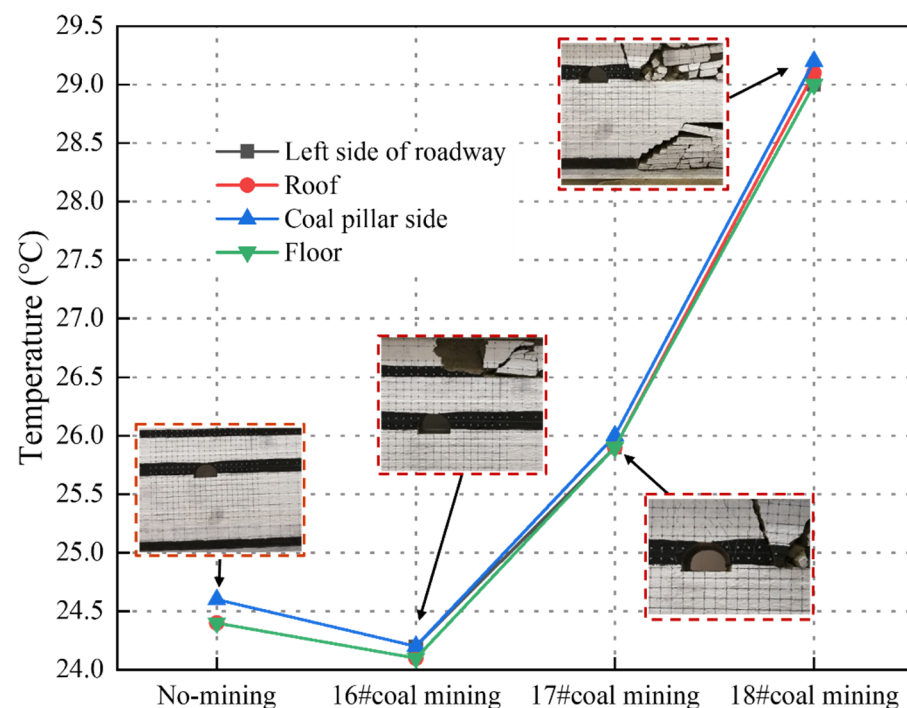


**Figure 12.** The temperature changes of the surrounding rock of the roadway at different locations during the mining of different coal seams.

Based on analysis on the experiment results, it can be seen that the temperature range of the surrounding rock was roughly symmetrically distributed when the roadway was not affected by the repeated mining in the close distance coal seams after excavation, and the temperature of the two sides of the roadway surrounding rock was higher than that of the other parts, which indicated that the stress was concentrated at the two sides of the roadway surrounding rock at this time. After the 16# coal above the roadway was mined, due to the impact of pressure relief of the upper coal seam mined, the stress transmitted from the coal pillar of the final mining line of 16# coal to the surrounding rock of the roadway decreased, resulting in a general decrease in the temperature of the surrounding rock of the roadway (to an average value of 24.1 °C). At this time, the stress concentration coefficient of the surrounding rock decreased. When the 17# coal was mined, the advance

support pressure of mining of the working face directly acts on the surrounding rock, resulting in a significant increase in the stress concentration range and strength of the surrounding rock, and a sharply increased in the temperature of the surrounding rock (up to the minimum value of 25.9 °C). Compared with the 16# coal was mined, its temperature increase is 1.8 °C, and compared with non-mined, it is 1.4 °C. The temperature on the right side of the roadway (near the coal pillar) was higher than that of other parts of the surrounding rock, indicating that the stress concentration on the side near the coal pillar was high, and the stress of the surrounding rock of the roadway presents an asymmetric distribution. When the 18# coal which is below the roadway was mined, affected by the repeated mining of upper two coal seams, the temperature of the surrounding rock raised to an average value of 29.1 °C, which was 3.2 °C higher than that of the 17# coal was mined. The stress concentration of the surrounding rock of the roadway continues to rise, and the temperature of the surrounding rock of the coal pillar side was still higher than that of the other parts, indicating that the stress concentration was still in the coal pillar side. According to the analysis of Figure 12, the temperature of both sides of the roadway was generally higher than that of the roof and floor before and after the mining of the coal seams. Additionally, the temperature of the coal pillar side was always the highest compared with other parts, indicating that the stress concentration of the two sides was high, while the stress of the coal pillar side was the most concentrated.

## 6. Conclusions

1. It puts forward an accurate laying of model and precise excavation of roadway test method named LPDLPRM which can effectively solve the problem of accurate laying of model and precise excavation of roadway in physical similarity simulation test of roadway with special surrounding rock structures. Additionally, the neat excavation of roadway outline can be realized by this method, so that the monitoring data are accurate and reliable, which can provide reference for the physical similarity simulation test of this kind of roadway.
2. Due to the influence of repeated mining disturbance, the cracks distribution of the surrounding rock of the coal-rock rise in the close distance coal seams shows the asymmetric characteristics and it was denser in coal pillar side than the other parts. With the lower coal seam being mined, the cracks of the surrounding rock increased gradually. Under this condition, measures should be taken to strengthen the support in coal pillar side and to control the asymmetric deformation.
3. Under the influence of repeated mining in the close distance coal seams, the stress concentration of roadway surrounding rock was weakened due to the pressure relief of upper coal seam being mined. The abutment pressure increased significantly when the coal seam and the lower coal seam were mined, resulting in a sharp stress increase in the surrounding rock, and seriously influenced on stability of roadway. Therefore, in the case of repeated mining, the support of the coal-rock rise should be strengthened in the mining process of the coal seam where the roadway was located and the lower coal seam working face.

## 7. Patents

This paper produced a patent: A physical similarity model for roadways or tunnels with special surrounding rock structures. The patent number is ZL202122187976.2.

**Author Contributions:** Conceptualization, P.L. (Pengze Liu) and L.G.; methodology, P.L. (Pengze Liu) and L.G.; software, P.Z. and Y.W.; validation, G.W., L.G. and P.L. (Pengze Liu); formal analysis, P.L. (Pengze Liu); investigation, P.L. (Pengze Liu), L.G., X.K., Z.M., D.K. and S.H.; resources, L.G.; data curation, P.L. (Pengze Liu); writing—original draft preparation, P.L. (Pengze Liu); writing—review and editing, L.G.; visualization, L.G. and P.L. (Pengze Liu); supervision, P.L. (Pengze Liu); project administration, P.L. (Pengze Liu); funding acquisition, L.G., X.K. and P.L. (Pengze Liu). All authors have read and agreed to the published version of the manuscript.

**Funding:** This research was funded by the National Natural Science Foundation of China (nos. 52004073 and 52064009); the Science and Technology Support Plan of Guizhou Province (no. Qian Ke He Zhi Cheng [2021] General 400); the Science and Technology Foundation of Guizhou Province (no. Qian Ke He Ji Chu [2020] 1Y216); the Guizhou Science and Technology Plan Project (Qianke Science Foundation [2020] 1Z047); the Scientific Research Project for Talents Introduction of Guizhou University (no. Gui Da Ren Ji He Zi (2020) no. 42); the Cultivation Project of Guizhou University (no. Guidapeiyu [2019] no. 27); the Open Project Fund of Key Laboratory of Mining Disaster Prevention and Control (no. SMDPC202106) during the research.

**Institutional Review Board Statement:** The study did not require ethical approval.

**Informed Consent Statement:** Informed consent was obtained from all subjects involved in the study.

**Data Availability Statement:** The data presented in this study are available on request from the corresponding author.

**Conflicts of Interest:** The authors declare no conflict of interest.

## References

- Zhang, P.D.; Gao, L.; Liu, P.Z.; Wang, Y.Y.; Liu, P.; Kang, X.T. Study on the influence of borehole water content on bolt anchoring force in soft surrounding rock. *Shock Vib.* **2022**, *2022*, 2384626. [CrossRef]
- Gao, L.; Zhao, S.H.; Huang, X.F.; Ma, Z.Q.; Kong, D.Z.; Kang, X.T.; Han, S. Experimental study on surrounding rock characteristics of gateway in Panjiang mining area. *J. GZU (Nat. Sci.)* **2022**, 1–6. Available online: <http://kns.cnki.net/kcms/detail/52.5002.N.20220412.0956.002.html> (accessed on 13 April 2022).
- Yu, Y.; Shen, W.L.; Guo, J. Deformation mechanism and control of lower seam roadway of contiguous seams. *J. Min. Saf. Eng.* **2016**, *33*, 49–55.
- Chai, J.; Du, W.G.; Yuan, Q.; Zhang, D.D. Study on the mechanism of rock mass fracture around high internal pressure roadway by establishing physical similarity model. *Opt. Fiber Technol.* **2019**, *48*, 84–94. [CrossRef]
- Guo, J.G.; Li, Y.H.; Shi, S.H.; Jiang, Z.S.; Chen, D.D.; He, F.L.; Xie, S.R. Self-forming roadway of roof cutting and surrounding rock control technology under thick and hard basic roof. *Journal of China Coal Society. J. China Coal Soc.* **2021**, *46*, 2853–2864.
- Chen, S.J.; Wang, H.L.; Zhang, J.W.; Xing, H.L.; Wang, H.Y. Experimental study on low-strength similar-material proportioning and properties for coal mining. *Adv. Mater. Sci. Eng.* **2015**, *2015*, 696501. [CrossRef]
- Li, L.; Wang, M.Y.; Fan, P.X.; Jiang, H.M.; Cheng, Y.H.; Wang, D.R. Strain rockbursts simulated by low-strength brittle equivalent materials. *Adv. Mater. Sci. Eng.* **2016**, *2016*, 5341904. [CrossRef]
- Kong, H.L.; Wang, H.Z.; Gu, G.Q.; Xu, B. Application of DICM on similar material simulation experiment for rocklike materials. *Adv. Civ. Eng.* **2018**, *2018*, 5634109.
- Mei, C.; Fang, Q.; Luo, H.W.; Yin, J.G.; Fu, X.D. A synthetic material to simulate soft rocks and its applications for model studies of socketed piles. *Adv. Civ. Eng.* **2017**, *2017*, 1565438. [CrossRef]
- Chen, X.G.; Wang, Y.; Mei, Y.; Zhang, X. Numerical simulation on zonal disintegration in deep surrounding rock mass. *Sci. World. J.* **2014**, *2014*, 379326. [CrossRef]
- Huang, F.; Zhu, H.H.; Xu, Q.W.; Cai, Y.C.; Zhuang, X.Y. The effect of weak interlayer on the failure pattern of rock mass around tunnel-Scaled model tests and numerical analysis. *Tunn. Undergr. Space Technol.* **2013**, *35*, 207–218. [CrossRef]
- Sterpi, D.; Cividini, A. A physical and numerical investigation on the stability of shallow tunnels in strain softening media. *Rock Mech. Rock Eng.* **2004**, *37*, 277–298. [CrossRef]
- Kong, D.Z.; Li, Q.; Wu, G.Y.; Song, G.F. Characteristics and control technology of face-end roof leaks subjected to repeated mining in close-distance coal seams. *Bull. Eng. Geol. Environ.* **2021**, *80*, 8363–8383. [CrossRef]
- Lin, J.; Wang, Y.; Yang, J.H.; Wang, Z.S.; Cai, J.F. Simulation studies on stress field evolution of roadway excavation under different confining pressures. *J. China Coal Soc.* **2015**, *40*, 2313–2319.
- Chen, X.G.; Zhang, Q.Y.; Liu, D.J.; Zhang, N.; Li, S.C. A3-D geomechanics model test study of the anchoring character for deep tunnel excavations. *Chin. Civ. Eng. J.* **2011**, *44*, 107–111.
- Jongpradist, P.; Tunsakul, J.; Kongkitkul, W.; Fadsiri, N.; Arangelovski, G.; Youwai, S. High internal pressure induced fracture patterns in rock masses surrounding caverns: Experimental study using physical model tests. *Eng. Geol.* **2015**, *197*, 158–171. [CrossRef]
- Yan, H.; Zhang, J.X.; Feng, R.M.; Wang, W.; Lan, Y.W.; Xu, Z.J. Surrounding rock failure analysis of retreating roadways and the control technique for extra-thick coal seams under fully-mechanized top caving and intensive mining conditions: A case study. *Tunn. Undergr. Space Technol.* **2020**, *97*, 103241. [CrossRef]
- Hui, G.L.; Niu, S.J.; Jing, H.W.; Wang, M. Physical simulation on deformation rules of god-side roadway subjected to dynamic pressure. *J. Min. Saf. Eng.* **2010**, *27*, 77–81+86.
- Mishra, S.; Kumar, A.; Rao, K.S.; Gupta, N.K. Experimental and numerical investigation of the dynamic response of tunnel in soft rocks. *Structures* **2021**, *29*, 2162–2173. [CrossRef]

20. Shan, R.L.; Huang, B.; Zheng, Y.; Kong, X.S.; Zhang, S.P.; Zhang, L.Z. Development of similar simulation equipment for roadway support subjected to vertical dynamic loads. *Chin. J. Geotech. Eng.* **2018**, *40*, 1163–1173.
21. Chang, J.C.; Li, D.; Xie, T.F.; Shi, W.B.; He, K. Deformation and failure characteristics and control technology of roadway surrounding rock in deep coal mines. *Geofluids* **2020**, *2020*, 8834347. [[CrossRef](#)]
22. Oh, D.W.; Lee, Y.J. Analysis of pile load distribution and ground behaviour depending on vertical offset between pile tip and tunnel crown in sand through laboratory model test. *J. Korean Tunn. Undergr. Space Assoc.* **2017**, *19*, 355–373. [[CrossRef](#)]
23. Li, Y.H.; Liu, D.Z.; Yang, S. Development and application of physical simulation test system for small and medium-sized tunnels based on biaxial motor loading. *Chin. J. Geot. Eng.* **2020**, *42*, 1556–1563.
24. Yuan, Z.G.; Shao, Y.H.; Zhu, Z.H. Similar Material Simulation Study on Protection Effect of Steeply Inclined Upper Protective Layer Mining with Varying Interlayer Distances. *Adv. Civ. Eng.* **2019**, *2019*, 9849635. [[CrossRef](#)]
25. Wang, Z.Y.; Dou, L.M.; He, J. Failure characteristics of rock bursts in steeply-inclined extra-thick coal seams under static-dynamic coupling loading. *J. Min. Saf. Eng.* **2021**, *38*, 886–894.
26. Idinger, G.; Aklík, P.; Wu, W.; Borja, R.I. Centrifuge model test on the face stability of shallow tunnel. *Acta Geotech.* **2011**, *6*, 105–117. [[CrossRef](#)]
27. He, M.C.; Gong, W.L.; Zhai, H.M.; Zhang, H.P. Physical modeling of deep ground excavation in geologically horizontal strata based on infrared thermography. *Tunn. Undergr. Space Technol.* **2010**, *25*, 366–376. [[CrossRef](#)]
28. Li, H.L.; Bai, H.B.; Ma, D.; Tian, C.D.; Zhang, Q. Physical simulation testing research on mining dynamic loading effect and induced coal seam floor failure. *J. Min. Saf. Eng.* **2018**, *35*, 366–372.
29. Ren, Y.F.; Ning, Y.; Qi, Q.X. Physical analogous simulation on the characteristics of overburden breakage at shallow longwall coalface. *J. China Coal Soc.* **2013**, *38*, 61–66.
30. Shi, X.S.; Jing, H.W.; Zhao, Z.L.; Gao, Y.; Zhang, Y.C.; Ruodi, B. Physical experiment and numerical modeling on the failure mechanism of gob-side entry driven in thick coal seam. *Energies* **2020**, *13*, 5425. [[CrossRef](#)]
31. Berthoz, N.; Branque, D.; Subrin, D.; Wong, H.; Humbert, E. Face failure in homogeneous and stratified soft ground: Theoretical and experimental approaches on 1g EPBS reduced scale model. *Tunn. Undergr. Space Technol.* **2012**, *30*, 25–37. [[CrossRef](#)]
32. Feng, C.; Dong, S.; Lai, X.P.; Chen, J.Q.; Cao, J.T.; Shan, P.F. Study on rule of overburden failure and rock burst hazard under repeated mining in fully mechanized top-coal caving face with hard roof. *Energies* **2019**, *12*, 4780.
33. Xue, J.H.; Wang, H.P.; Zhou, W.; Ren, B.; Duan, C.R.; Deng, D.S. Experimental research on overlying strata movement and fracture evolution in pillarless stress-relief mining. *Int. J. Coal Sci. Technol.* **2015**, *2*, 38–45. [[CrossRef](#)]
34. Yang, K.; He, X.; Dou, L.T.; Liu, W.J.; Sun, L.; Ye, H.S. Experimental investigation into stress-relief characteristics with upward large height and upward mining under hard thick roof. *Int. J. Coal Sci. Technol.* **2015**, *2*, 91–96. [[CrossRef](#)]
35. Zhang, S.K.; Lu, L.; Wang, Z.M.; Wang, S.D. A physical model study of surrounding rock failure near a fault under the influence of footwall coal mining. *Int. J. Coal Sci. Technol.* **2021**, *8*, 626–640. [[CrossRef](#)]
36. Liu, P.Z.; Gao, L.; Zhang, P.D.; Wu, G.Y.; Wang, C.; Ma, Z.Q.; Kong, D.Z.; Kang, X.T.; Han, S. A case study on surrounding rock deformation control technology of gob-side coal-rock roadway in inclined coal seam of a mine in Guizhou, China. *Processes* **2022**, *10*, 863. [[CrossRef](#)]
37. Gao, L.; Liu, P.Z.; Zhang, P.D.; Wu, G.Y.; Kang, X.T. Influence of fracture types of main roof on the stability of surrounding rock of the gob-side coal-rock roadway in inclined coal seams and its engineering application. *Geol. Explor.* **2022**, 1–8. Available online: <https://kns.cnki.net/kcms/detail/61.1155.p.20220416.0838.002.html> (accessed on 5 April 2022).
38. Kong, D.Z.; Xiong, Y.; Cheng, Z.B.; Wang, N.; Wu, G.Y.; Liu, Y. Stability analysis of coal face based on coal face-support-roof-system in steeply inclined coal seam. *Geomech. Eng.* **2021**, *25*, 233–243.
39. Ji, Y.M. Study on Infrared Characteristics of Bolt and Rock in Condition of Loading. *Spectrosc. Spectr. Anal.* **2010**, *30*, 659–662.
40. Toubal, L.; Karama, M.; Lorrain, B. Damage evolution and infrared thermography in woven composite laminates under fatigue loading. *Int. J. Fat.* **2006**, *28*, 1867–1872. [[CrossRef](#)]
41. Yang, Z.; Qi, Q.J.; Ye, D.D.; Li, X.; Luo, H. Variation of internal infrared radiation temperature of composite coal-rock fractured under load. *J. China Coal Soc.* **2016**, *41*, 618–624.
42. Peng, Y.Y.; Lin, Q.C.; He, M.C.; Zhu, C.; Zhang, H.J.; Guo, P.F. Experimental study on infrared temperature characteristics and failure modes of marble with prefabricated holes under uniaxial compression. *Energies* **2021**, *14*, 713. [[CrossRef](#)]
43. Ma, L.Q.; Li, Q.Q.; Cao, X.Q.; Zhou, T. Variation characteristics of internal infrared radiation temperature of coal-rock mass in compression process. *J. China Univ. Min. Technol.* **2013**, *42*, 331–336.
44. Meola, C. A new approach for estimation of defects detection with infrared thermography. *Mater. Lett.* **2007**, *61*, 747–750. [[CrossRef](#)]
45. Liu, S.J.; Wu, L.X.; Wu, H.P.; Wu, Y.H.; Cheng, T.; Li, G.H. Quantitative studies of infrared radiation dark mineral uniaxial loading process. *Chin. J. Rock Mech.* **2002**, *21*, 1585–1589.